4988 *Organometallics* **2009,** *28,* 4988–4995
DOI: 10.1021/om900497q

ORGANOMETALLICS
Article

Influence of *syn* and *anti* Configurations of NHC Backbone on Ru-Catalyzed Olefin Metathesis

Fabia Grisi,*[,†] Annaluisa Mariconda,[†] Chiara Costabile,[†] Valerio Bertolasi,[‡] and Pasquale Longo[†]

[†]*Dipartimento di Chimica, Universitá di Salerno, Via Ponte Don Melillo, I-84084 Fisciano, Salerno, Italy, and* [‡]*Dipartimento di Chimica and Centro di Strutturistica Diffrattometrica, Università di Ferrara, Via L. Borsari 46, I-44100 Ferrara, Italy*

Received June 12, 2009

The synthesis and characterization of two ruthenium-based olefin metathesis catalysts bearing N-heterocyclic carbene (NHC) ligands with *syn* (**12**) and *anti* (**13**) methyl groups on the backbone and *o*-tolyl *N*-substituents are reported. The catalytic performance of both **12** and **13** has been evaluated in ring-closing metathesis, ring-opening metathesis polymerization, and cross-metathesis reactions. The results have been compared to those obtained in the presence of the Grubbs second-generation catalyst **3a**, lacking substituents on the NHC backbone. Of particular interest, compound **12** outperformed both **3a** and **13** in the ring-closing metathesis of hindered olefins, demonstrating to be the most active monophosphine catalyst in this class of metathesis reactions up to now. The influence of *syn* and *anti* stereochemical relationship of methyl groups on the NHC backbone of **12** and **13** in the formation of sterically encumbered olefins has been discussed. The X-ray structure of novel ruthenium complex **15**, generated during an attempt to prepare pyridine-based complex **14** and identified as a decomposition product derived from C−H activation of *N*-tolyl substituents, is also reported.

Downloaded by UNIV DEGLI STUDI DI SALERNO at 08:51:29:159 on June 25, 2019
from https://pubs.acs.org/doi/10.1021/om900497q.

Introduction

Ruthenium-catalyzed olefin metathesis represents a privileged, effective means for constructing carbon−carbon double bonds in both organic synthesis and polymer chemistry.[1] The large success of ruthenium carbene complexes as olefin metathesis initiators is principally due to their high functional group tolerance in combination with high catalytic efficiency.[2] Following the initial report of Grubbs' first-generation catalyst (**1** in Chart 1),[3] much attention has been focused on the development of Ru-based catalysts with enhanced reactivity and stability. The replacement of one phosphine ligand by an N-heterocyclic carbene (NHC) moiety[4] paved the way for the burgeoning of new-generation catalysts (e.g., **2a** and **2b** in Chart 1) that in most applications have exhibited better performances than the diphosphine catalyst **1**.[5]

Among these, a series of NHC Ru catalysts with reduced bulk at the *ortho* positions of *N*-aromatic groups (e.g., **3a** and **3b** in Chart 1) have proved to be effective for the preparation of sterically encumbered olefins, which has so far represented a very challenging task for this class of catalysts.[6] The removal of one *ortho* substituent on each *N*-bound aryl ring of catalyst appears to be indispensable for allowing access to the ring-closing metathesis (RCM) and cross-metathesis (CM) of hindered substrates. Improved levels of reactivity in the formation of highly substituted olefins have been achieved by employing Ru catalysts possessing unsubstituted *N*-phenyl groups on the NHC ligand (**4** in Scheme 1).[6a] However, they are rather unstable and evolve to degradation products through *ortho* C−H activation of the *N*-phenyl groups (**4a**,**4b** in Scheme 1)[7]

The introduction of bulky substituents on the backbone of the NHC ligand stabilizes this class of complexes toward decomposition via C−H activation processes by restricting

*Corresponding author. E-mail: fgrisi@unisa.it.

(1) For selected reviews on olefin metathesis, see: (a) Füstner, A. *Angew. Chem., Int. Ed.* **2000**, *39*, 3012–3043. (b) Buchmeiser, M. R. *Chem. Rev.* **2000**, *100*, 1565–1604. (c) Grubbs, R. H. *Handbook of Olefin Metathesis*; Wiley-VCH: Weinheim, 2003. (d) Schrock, R. R.; Hoveyda, A. H. *Angew. Chem., Int. Ed.* **2003**, *42*, 4592–4633. (e) Grubbs, R. H. *Tetrahedron* **2004**, *60*, 7117–7140. (f) Astruc, D. *New J. Chem.* **2005**, *29*, 42–56. (g) Schrock, R. R. *Angew. Chem., Int. Ed.* **2006**, *45*, 3748–3759. (h) Grubbs, R. H. *Angew. Chem., Int. Ed.* **2006**, *45*, 3760–3765. (i) Deshmukh, P. H.; Blechert, S. *Dalton Trans.* **2007**, 2479–2491. (j) Hoveyda, A. H.; Zhugralin, A. R. *Nature* **2007**, *450*, 243–251.

(2) Trnka, T. M.; Grubbs, R. H. *Acc. Chem. Res.* **2001**, *34*, 18−29.

(3) Schwab, P.; Grubbs, R. H.; Ziller, J. W. *J. Am. Chem. Soc.* **1996**, *118*, 100–110.

(4) Scholl, M.; Ding, S.; Lee, C. W.; Grubbs, R. H. *Org. Lett.* **1999**, *1*, 953–956.

(5) (a) Weskamp, T.; Schattenmann, W. C.; Spiegler, M.; Hermann, W. A. *Angew. Chem., Int. Ed.* **1998**, *37*, 2490–2493. (b) Weskamp, T.; Kohl, F. J.; Hieringer, W.; Gleich, D.; Hermann, W. A. *Angew. Chem., Int. Ed.* **1999**, *38*, 2416–2419. (c) Huang, J.; Stevens, E. D.; Nolan, S. P.; Peterson, J. L. *J. Am. Chem. Soc.* **1999**, *121*, 2674–2678. (d) Füstner, A.; Ackermann, L.; Gabor, B.; Goddard, R.; Lehmann, C. W.; Mynott, R.; Stelzer, F.; Thiel, O. R. *Chem.—Eur. J.* **2001**, *7*, 3236–3253.

(6) (a) Berlin, J. M.; Campbell, K.; Ritter, T.; Funk, T. W.; Chlenov, A.; Grubbs, R. H. *Org. Lett.* **2007**, *9*, 1339–1342. (b) Stewart, I. C.; Ung, T.; Pletnev, A. A.; Berlin, J. M.; Grubbs, R. H.; Schrodi, Y. *Org. Lett.* **2007**, *9*, 1589–1592. (c) Stewart, I. C.; Campbell, K.; Grubbs, R. H. *Org. Lett.* **2008**, *10*, 441–444. (d) White, D. E.; Stewart, I. C.; Grubbs, R. H.; Stoltz, B. M. *J. Am. Chem. Soc.* **2008**, *130*, 810–811. (e) Chung, C. K.; Grubbs, R. H. *Org. Lett.* **2008**, *10*, 2693–2696.

(7) Hong, S. H.; Chlenov, A.; Day, M. W.; Grubbs, R. H. *Angew. Chem., Int. Ed.* **2007**, *46*, 5148–5151.

 Published on Web 08/18/2009 © 2009 American Chemical Society

Chart 1

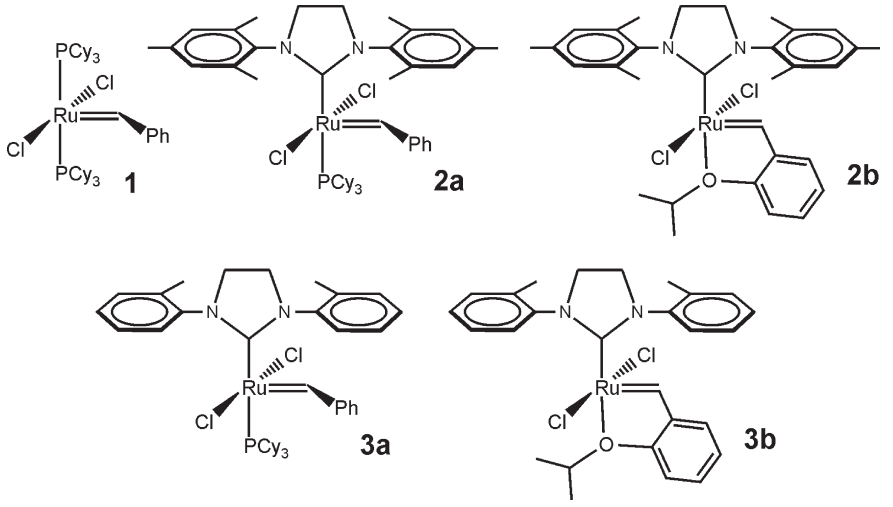

Scheme 1. Evolution to Degradation Products through *ortho* C−H Activation of the *N*-Phenyl Groups of Complex 4

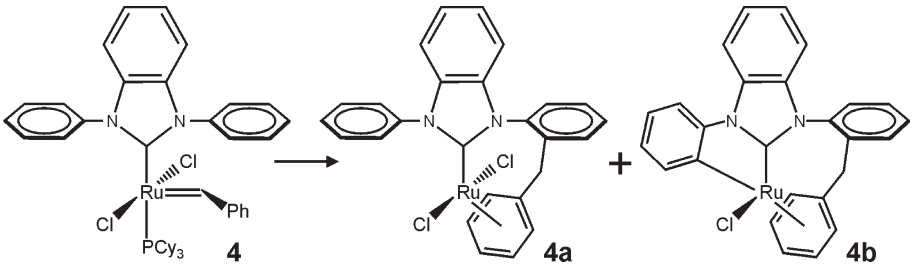

rotation of the *N*-aryl groups of the NHC ligand (**5** in Chart 2).[6e]

As a part of efforts for better understanding the role of NHC backbone substitution in addressing activity, stability, and selectivity of corresponding ruthenium catalysts, we report herein the synthesis and characterization of two new monophosphine ruthenium complexes (**12** and **13** in Scheme 2) bearing an NHC ligand with tolyl groups at nitrogen and methyl substituents in a *syn* and *anti* relationship on the backbone. We have recently reported the preparation and catalytic behavior in olefin metathesis of Ru complexes containing NHC ligands with *syn* and *anti* methyl groups on the backbone and bearing *N*-(*S*)-phenylethyl groups.[8]

The catalytic properties of **12** and **13** in olefin metathesis in relation to the *syn* and *anti* NHC-backbone substitution were evaluated and compared to those of complex **3a**, containing an NHC ligand lacking any substituents on the backbone. It is worth underlining that very recently Grubbs and co-workers have reported an elegant study on olefin metathesis promoted by a homologous series of phosphine-free ruthenium catalysts bearing NHCs with varying degrees of backbone and aryl substitution.[9] However, the ruthenium complex bearing an NHC ligand with methyl groups on the backbone and *o*-tolyl groups at the nitrogen is only reported as a mixture of *syn* and *anti* isomers and not yet investigated as an olefin metathesis initiator.

Chart 2

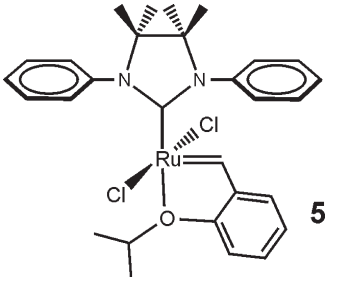

Results and Discussion

Synthesis of complexes **12** and **13** is described in Scheme 2. Starting diamines **6** and **7** were prepared according to a published procedure[10] and subsequently coupled to *o*-tolyl groups by Pd-catalyzed reaction to give diamines **8** and **9**. Dihydroimidazolium salts **10** and **11** were obtained by salification of **8** and **9** with HCl, followed by condensation with triethyl orthoformate. The corresponding free carbenes were generated in situ by treatment of these salts with potassium hexamethyldisilazide (KHMDS) at room temperature and then reacted with $(PCy_3)(Cl)_2Ru{=}CHPh$ to afford the desired complexes **12** and **13**.[6b] Both **12** and **13** are isolated as air- and moisture-stable solids after flash chromatography and fully characterized by ^{1}H, ^{13}C, and ^{31}P NMR.

(8) Grisi, F.; Costabile, C.; Gallo, E.; Tedesco, C.; Longo, P. *Organometallics* **2008**, *27*, 4647–4656.

(9) Kuhn, K. M.; Bourg, J.-B.; Chung, C. K.; Virgil, S. C.; Grubbs, R. H. *J. Am. Chem. Soc.* **2009**, *131*, 5313–5320.

(10) Chooi, S. Y. M.; Leung, P.; Ng, S.; Quek, G. H.; Sim, K. Y. *Tetrahedron Asymmetry* **1991**, *2*, 981–982.

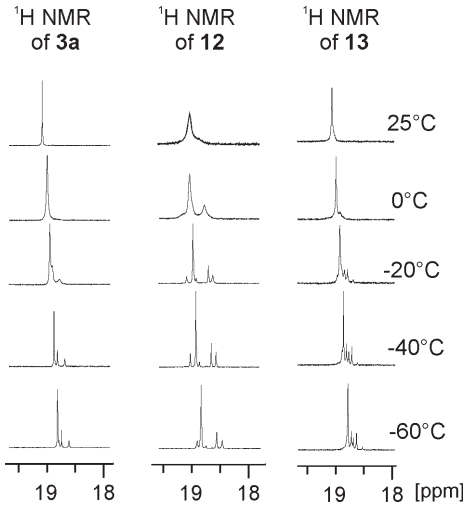

Figure 1. VT ^{1}H NMR experiments on complexes **3a**, **12**, and **13**.

Scheme 2. Synthesis of 12 and 13

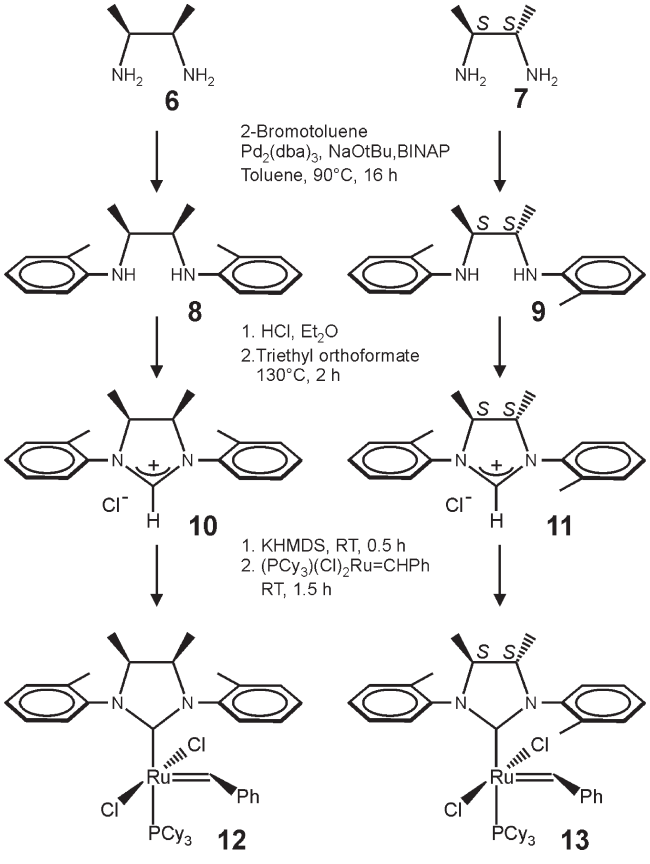

The presence of at least two isomers at RT for complex **12** is attested by ^{1}H, ^{13}C, and ^{31}P NMR spectra. Variable-temperature (VT) ^{1}H NMR experiments in the range -60 °C $< T <$ 25 °C show at least five isomers in solution at low T, by revealing five peaks for the alkylidene proton of the complex (Figure 1). Due to the symmetry of **12**, in frozen condition, eight diastereoisomers (and the corresponding eight enantiomers) are in principle possible. The five isomers observed by NMR at low T indicate that the other possible three isomers should present higher energy. Indeed, considering the possible rotations within **12** (θ, ϕ, τ1, and τ2 in Chart 3), even if only one among those would be unfrozen, we should observe not more than four isomers (for further details see Figure S1 of the Supporting Information). The NMR evidence of at least five isomers attests that all possible internal rotations, which cause the collapse of a couple of conformers, are frozen. The presence of at least two conformers at RT could be attributed to the activation of at least two rotations of Chart 3. On the basis of our data it is not possible to define which rotations are involved.

Chart 3

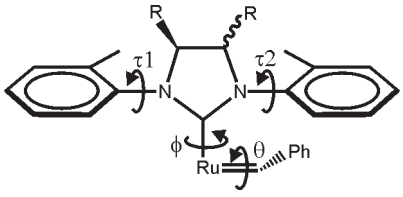

As for **13**, eight diastereoisomers are in principle possible in frozen condition. ^{1}H NMR spectra indicate the presence of at least six conformers at $T \leq -30$ °C, showing that also in this case all possible internal rotations (reported in Chart 3) are frozen. The presence of two conformers at 25 °C could be attributed, as well, to the activation of at least two rotations of Chart 3.

Finally, we investigated the behavior at VT of **3a**. The four diastereoisomers, in principle possible in frozen condition, are observed below -50 °C. All conformers collapse in one species at RT, indicating that besides the ϕ and θ rotations, at least one between τ1 and τ2 has to be active (see Supporting Information for further details).

These observations lead to the conclusion that the methyl groups on the backbone in **12** and **13** are probably responsible for a high-energy barrier rotation of the tolyl groups around τ1 and τ2, hampering the presence of only one species at RT.

Crystals of **12** suitable for X-ray structure analysis were grown by vapor diffusion of pentane into a saturated benzene solution at room temperature. ORTEP[11] views **a** and **b** of complex **12**, displaying the two conformations of the disordered *o*-tolyl N1 substituent, with occupation factors of 0.62/0.38, are shown in Figure 2. The Ru center is pentacoordinated, and the complex adopts a square-pyramidal geometry. The two chlorine atoms are *trans*-oriented in the basal plane of the square pyramid, with the phosphorus and the imidazolyl carbon atoms occupying the remaining sites. The benzylidene carbene ligand is situated in the apical position. The Ru atom is positioned 0.23 Å above the basal plane toward the C20 carbene atom. The phenyl ring belonging to the benzylidene ligand is almost coplanar with the *o*-tolyl N1 substituent at the N-heterocyclic carbene with tilt angles of 14.4(1)° and 17.4(2)° for the C6/C12 and C6′/C12′ conformers, respectively. The distances between the centroids of these almost parallel rings of 3.88(1) and 3.91(1) Å are indicative of rather weak $\pi-\pi$ interactions. The *o*-tolyl *N*-substituents are twisted with respect to the NHC ring by 67.2(1)° for the C13/C19 group and 80.1(1)−86.2(2)° for the C6/C12 and C6′/C12′ disordered moieties. The dihedral angle between the C1−Ru1−Cl2 and Ru1=C20−C21 planes is 36.5(2)°. The other structural parameters are very similar with respect to

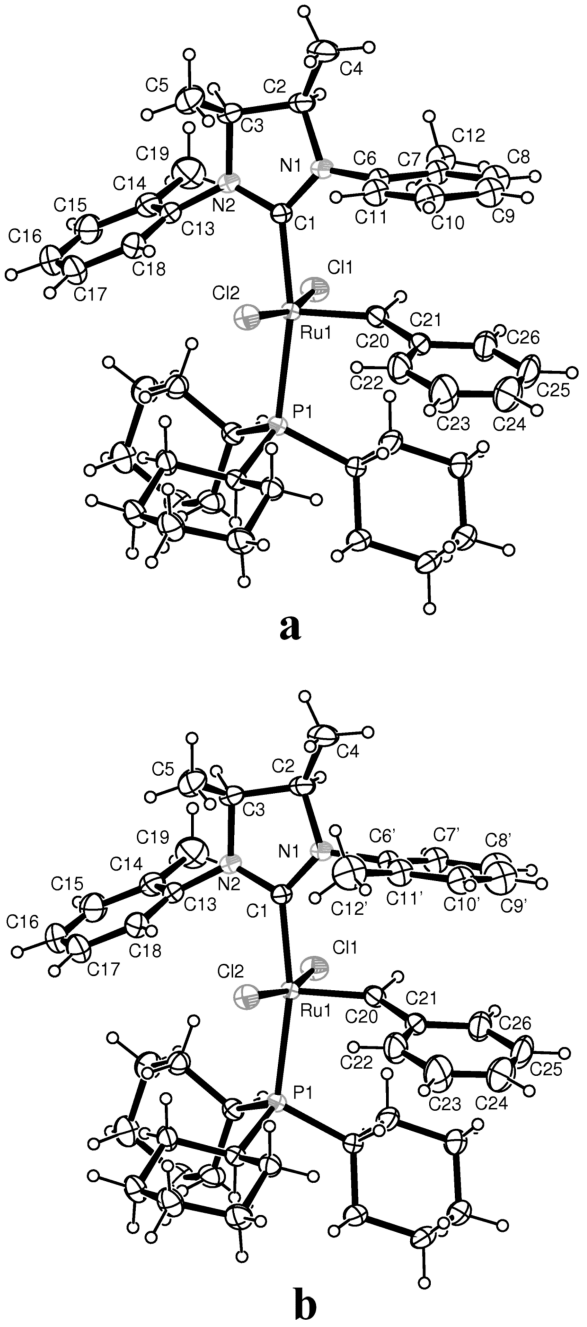

Figure 2. ORTEP[11] views, **a** and **b**, of complex **12**, displaying the two conformations of disordered *o*-tolyl N1 substituent, with occupation factors of 0.62/0.38.

Chart 4

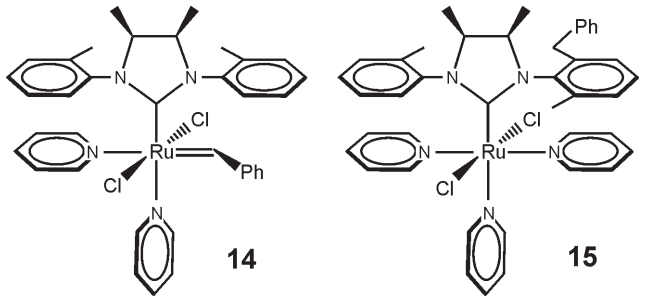

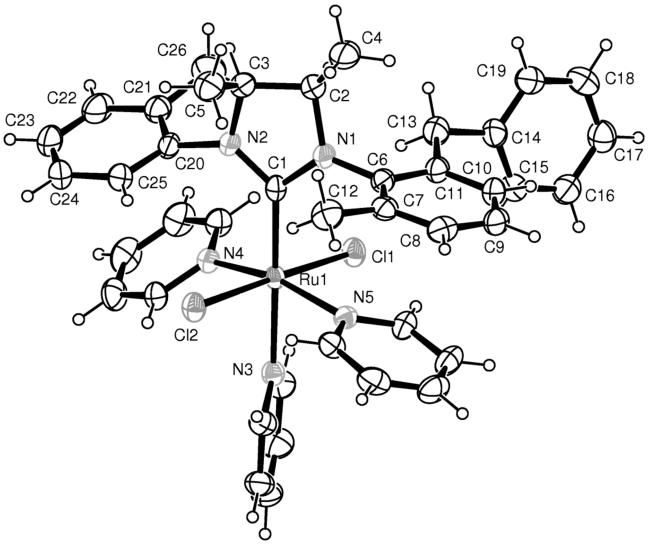

Figure 3. X-ray crystallographic analysis of **15**.

those observed in many other analogue complexes that differ only in the NHC substituents.[5d,12−16]

Unfortunately, only crystals of very poor resolution could be grown of complex **13**.

Both **12** and **13** are quite stable in solution, as shown by monitoring the retention of the benzylidene signal by ^{1}H NMR spectroscopy over the course of one week. According to Grubbs and co-workers, the presence of methyl substituents on the backbone of the NHC ligand of complexes **12** and **13** helps to prevent catalyst decomposition via C−H activation processes, because the restriction of *N*-aryl group rotation hinders the necessary proximity of an aryl C−H bond and the ruthenium center.[6a,6e] Interestingly, in an attempt to synthesize the bispyridine-based catalyst **14** by treating **12** with an excess of pyridine in toluene,[17] we observed the tris(piridyne) complex **15** as a decomposition product (Chart 4). The structure of **15** was elucidated by X-ray crystallographic analysis (Figure 3).

The complex displays an octahedral geometry where two chlorine atoms and two pyridine rings are in mutual *trans* positions. The third pyridine ring is in *trans* position with respect to the NHC derivative. The NHC is unsymmetrically N-disubstituted by two different phenyl derivatives, the *o*-tolyl group and the 2-methyl-6-benzylphenyl substituent, derived from the decomposition of the Ru-benzylidene moiety. The *N*-phenyl rings C6/C10 and C20/C25 are rotated by 83.9(1)° and 69.8(1)° with respect to the NHC ring and are almost parallel to N5/C41 and N4/C36 pyridine rings with tilt angles of 10.0(1)° and 19.4(1)°, respectively. The distances between the centroids of both ring couples C6/C11, N5/C41 and C20/C25, N4/C36 of 3.449(5) and 3.451(5) Å

(11) Burnett, M. N.; Johnson, C. K. *ORTEP III*, Report ORNL-6895; Oak Ridge National Laboratory: Oak Ridge, TN, 1996.
(12) Fürstner, A.; Krause, H.; Ackermann, L.; Lehmann, C. W. *Chem. Commun.* **2001**, 2240–2241.
(13) Dinger, M. B.; Nieczypor, P.; Mol, J. C. *Organometallics* **2003**, *22*, 5291–5296.
(14) Love, J. A.; Sanford, M. S.; Day, M. W.; Grubbs, R. H. *J. Am. Chem. Soc.* **2003**, *125*, 10103–10109.
(15) Prühs, S.; Lehmann, C. W.; Fürstner, A. *Organometallics* **2004**, *23*, 280–287.
(16) Vougioukalakis, G. C.; Grubbs, R. H. *Organometallics* **2007**, *26*, 2469–2472.
(17) Sanford, M. S.; Love, J. A.; Grubbs, R. H. *Organometallics* **2001**, *20*, 5314–5318.

Scheme 3. RCM of Substrates 16, 18, and 20

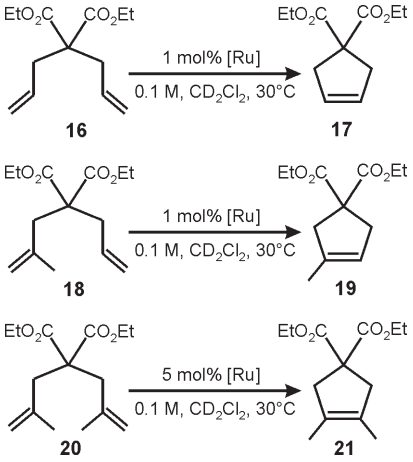

reveal the presence of quite efficient $\pi-\pi$ interactions. All bond distances and angles are typical and very similar to those observed in the other analogous octahedral structure of $(H_2IMes)(Py)_3Cl_2Ru$ complex[18] (H_2IMes = 1,3-dimesityl-4,5-dihydroimidazol-2-ylidene).

The crystal structure is consistent with a degradation product deriving from the insertion of the benzylidene carbon atom of **12** into the *ortho* C−H bond of one of the *N*-tolyl rings of the NHC ligand. Although both experimental and theoretical studies have been recently devoted to shed light on the decomposition mechanisms of Grubbs second-generation catalysts,[7,18,19] the deactivation pathway of pyridine-containing catalysts is not at all elucidated, the role of pyridine in this process being unclear.[18,20] The decomposition reaction of complex **12** in the presence of pyridine is still under study .

The catalytic behavior of new complexes **12** and **13** was investigated by using a standard set of metathesis reactions.[21]

We initially studied the catalytic activity of **12** and **13** in the ring-closing metathesis of diethyl diallylmalonate **16**, diethyl allylmethallylmalonate **18**, and diethyl dimethallylmalonate **20** (Scheme 3, Table 1). All the reactions were monitored by ^{1}H NMR spectroscopy, and the related plots of product concentration vs time are depicted in Figures 4−6.

In the ring-closing metathesis of **16**, conducted in the presence of 1 mol % of catalyst in CD_2Cl_2 at 30 °C, complex

Table 1. RCM, ROMP, and CM Conducted in the Presence of 2a, 3a, 12, and 13

entry	cat	substrate	product	*t* (h)	yield %[a]	*E*:*Z*[b]
1[c]	**3a**	**16**	**17**	1	98	
2[c]	**12**	**16**	**17**	1	98	
3[c]	**13**	**16**	**17**	1	92	
4[c]	**3a**	**18**	**19**	1	84	
5[c]	**12**	**18**	**19**	1	90	
6[c]	**13**	**18**	**19**	1	80	
7[d]	**3a**	**20**	**21**	1	70	
8[d]	**12**	**20**	**21**	1	82	
9[d]	**13**	**20**	**21**	1	47	
10[e]	**2a**	**22**	poly(**22**)	0.15	100	1.6
11[e]	**3a**	**22**	poly(**22**)	0.11	100	1.3
12[e]	**12**	**22**	poly(**22**)	0.11	100	1.9
13[e]	**13**	**22**	poly(**22**)	0.13	100	1.3
14[f]	**2a**	**22**	poly(**22**)	0.68	100	1.1
15[f]	**3a**	**22**	poly(**22**)	0.53	100	1.0
16[f]	**12**	**22**	poly(**22**)	0.51	> 98	0.8
17[f]	**13**	**22**	poly(**22**)	0.54	> 98	0.8
18	**2a**	**23**, **24**	**25**	12	80	7 [25]
19[g]	**3a**	**23**, **24**	**25**	12	60	8.0[e]
20[g]	**12**	**23**, **24**	**25**	12	62	8.9[e]
21[g]	**13**	**23**, **24**	**25**	12	68	7.0[e]

[a] Determined by NMR. [b] Ratio based on data from ^{1}H and ^{13}C NMR of isolated products. [c] Reaction conducted in CD_2Cl_2, at 30 °C, catalyst 1 mol %, **16** and **18** 0.1 M. [d] Reaction conducted in CD_2Cl_2, at 30 °C, catalyst 5 mol %, **20** 0.1 M. [e] Reaction conducted in CD_2Cl_2, at 30 °C, catalyst 0.01 mol %, **22** 0.5 M. [f] Reaction conducted in CD_2Cl_2, at 30 °C, catalyst 0.1 mol %, **22** 0.5 M. [g] Reaction conducted in CH_2Cl_2, at 40 °C, catalyst 2.5 mol %, **23** 0.2 M.

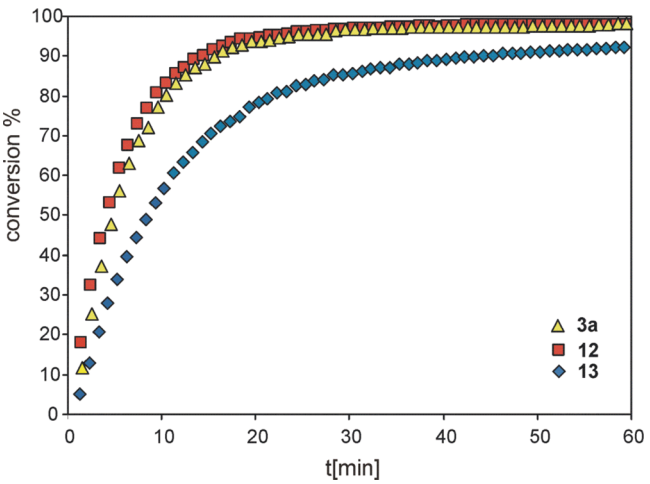

Figure 4. Kinetic profiles of RCM of **16** in the presence of **3a**, **12**, and **13**.

12 efficiently cyclized **16**, with very similar activity to that of catalyst **3a** (> 98% conversion within 60 min), whereas complex **13** performed the same reaction with slightly slower rate (92% conversion in 60 min) (Figure 4).

The RCM of diethyl allylmethallylmalonate **18** leads to the formation of cyclopentene **19**, featuring a trisubstituted double bond (Scheme 3, Table 1). Due to steric effects, this reaction is more demanding than the corresponding RCM of **16** and, for this reason, better highlights small differences in catalyst activity. Indeed, in the RCM of **18** (1 mol % catalyst loading, 30 °C, CD_2Cl_2), a clear distinction between complexes **12** and **13** has begun to emerge, as sketched in Figure 5. Moreover, complex **12** showed the highest activity, slightly surpassing catalyst **3a** in efficiency.

(18) Hong, S. H.; Wenzel, A. G.; Salguero, T. T.; Day, M. W.; Grubbs, R. H. *J. Am. Chem. Soc.* **2007**, *129*, 7961–7068.
(19) (a) Ulman, M.; Grubbs, R. H. *J. Org. Chem.* **1999**, *64*, 7202–7207. (b) Sanford, M. S.; Love, J. A.; Grubbs, R. H. *J. Am. Chem. Soc.* **2001**, *123*, 6543–6554. (c) Trnka, T. M.; Morgan, J. P.; Sanford, M. S.; Wilhelm, T. E.; Scholl, M.; Choi, T.; Ding, S.; Day, M. W.; Grubbs, R. H. *J. Am. Chem. Soc.* **2003**, *125*, 2546–2558. (d) Hong, S. H.; Day, M. W.; Grubbs, R. H. *J. Am. Chem. Soc.* **2004**, *126*, 7414–7415. (e) Dinger, M. B.; Mol, J. C. *Organometallics* **2003**, *22*, 1089–1095. (f) Dinger, M. B.; Mol, J. C. *Eur. J. Inorg. Chem.* **2003**, 2827. (g) Hong, S. H.; Day, M. W.; Grubbs, R. H. *J. Am. Chem. Soc.* **2004**, *126*, 7414–7415. (h) Galan, B. R.; Gembicky, M.; Dominiak, P. M.; Keister, J. B.; Diver, S. T. *J. Am. Chem. Soc.* **2005**, *127*, 15702–15703. (i) Vehlow, K.; Gessler, S.; Blechert, S. *Angew. Chem., Int. Ed.* **2007**, *46*, 8082–8085. (j) Mathew, J.; Koga, N.; Suresh, C. H. *Organometallics* **2008**, *27*, 4666–4670. (k) Leitao, E. M.; Dubberley, S. R.; Piers, W. E.; Wu, Q.; McDonald, R. *Chem.—Eur. J.* **2008**, *14*, 11565–11572. (l) Galan, B. R.; Pitak, M.; Gembicky, M.; Keister, J. B.; Diver, S. T. *J. Am. Chem. Soc.* **2009**, *131*, 6822–6832.
(20) Williams, J. E.; Harner, M. J.; Sponsler, M. B. *Organometallics* **2005**, *24*, 2013–2015.
(21) Ritter, T.; Hejl, A.; Wenzel, A. G.; Funk, T. W.; Grubbs, R. H. *Organometallics* **2006**, *25*, 5740–5745.

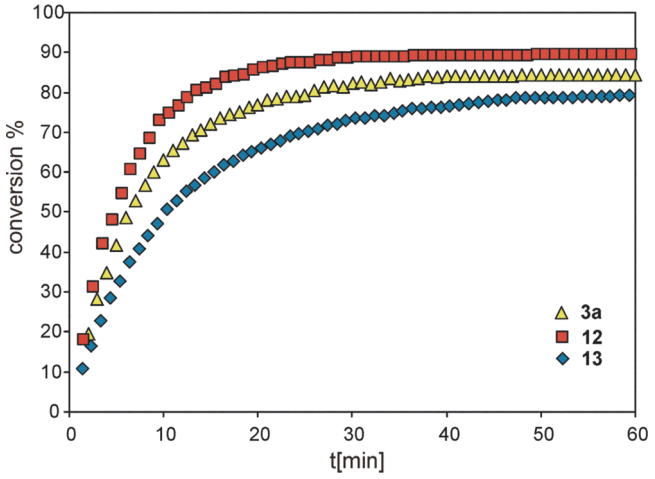

Figure 5. Kinetic profiles of RCM of **18** in the presence of **3a**, **12**, and **13**.

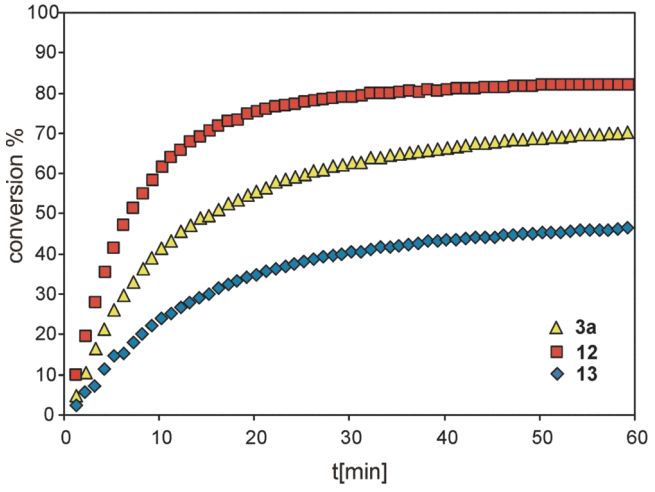

Figure 6. Kinetic profiles of RCM of **20** in the presence of **3a**, **12**, and **13**.

Scheme 4. ROMP of 22

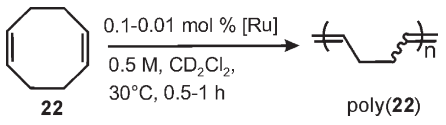

The same trend, even if with slower reaction rates, was observed when more challenging substrate **20** was employed (Scheme 3,Table 1). The results for the RCM of **20**, performed by utilizing a catalyst loading of 5 mol % in CD_2Cl_2 at 30 °C, are depicted in Figure 6. Complex **12** outperformed once again both **3a** and **13**, furnishing the cycloalkene **21** in 82% yield within 60 min. To the best of our knowledge, complex **12** is the most active monophosphine-ruthenium catalyst for the RCM of the hindered substrate **20** at 30 °C. More interestingly, the latter RCM reaction has displayed a more marked difference in activity between catalyst **12** and **13** than the previous case. Judging from the results described so far, one can easily infer that the role of NHC-backbone substitution is crucial in determining RCM behavior of complexes **12** and **13**, as underlined by comparing the activities of **12** and **13** to that of catalyst **3a** (see Figures 4−6).

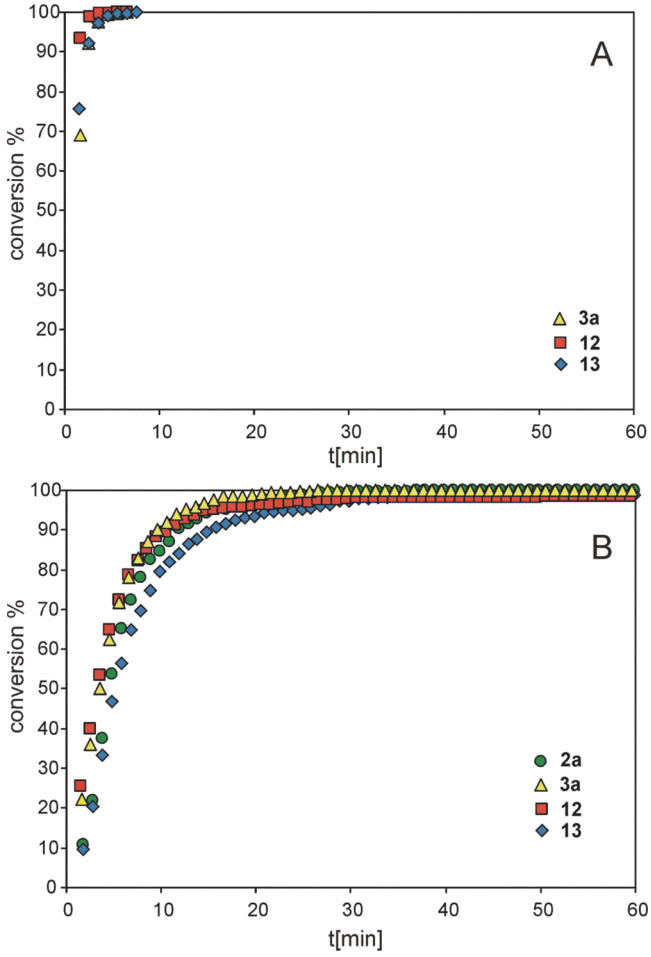

Figure 7. Kinetic profiles of ROMP of 1,5-cyclooctadiene (COD) **22** in the presence of 0.1 mol % (profile A) and 0.01 mol % (profile B) of catalyst.

Chart 5. Double Views of 12 and 13[a]

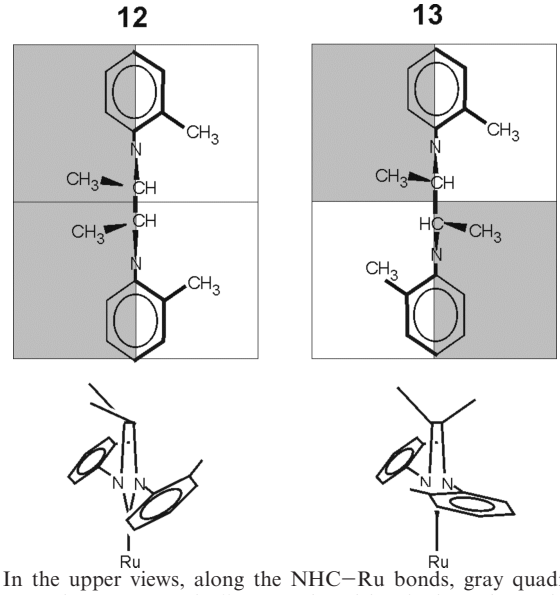

[a] In the upper views, along the NHC−Ru bonds, gray quadrants correspond to zones sterically encumbered by the bent down side of N-bonded aromatic rings.

Indeed, complexes **12** and **13** differ only in the relative orientation of the methyl groups on the NHC-backbone

Scheme 5. CM of Substrates 23 and 24

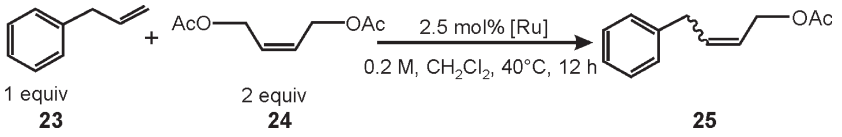

(*syn* for **12** and *anti* for **13**, respectively), a fact that excludes electronic factors from any speculation about the rationalization of their different catalytic performance. A logical interpretation of the experimental data can be given by invoking steric factors. Very likely, the different reactivities in RCM observed for **12** and **13** can be justified by considering that the relative disposal of methyl groups on the backbone influences the conformation of the *N*-aryl rings of the NHC, defining a differently encumbered active space at the metal (Chart 5). More in detail, as reported for **3a** by Grubbs and co-workers,[22] the high reactivity observed for catalyst **12** can be due to accessibility of conformations in which the *N*-aryl rings are rotated away from approaching and coordinated olefins, as a consequence of a preferential *syn* orientation displayed by *N*-tolyl rings. In particular, as for **12**, the *syn* orientation of the *N*-tolyl rings would be even more favored due to *syn* orientation of backbone methyl substituents. It is worth noting that the most hindered catalyst side would be represented, in this hypothesis, by the part of the space where methyl groups on the backbone are oriented and not by the space occupied by the *ortho*-methyl substituents, as one could intuitively suppose.[23]

Afterward, we tested the catalytic activity of **12** and **13** in the ROMP of 1,5-cyclooctadiene (COD) **22** (Scheme 4, Table 1). Figure 7 displays the kinetics of ROMP of **22** to form poly(**22**) in the presence of 0.1 mol % (profile A) and 0.01 mol % (profile B) of catalyst. Both **12** and **13** are efficient catalysts for the polymerization of **22**, reaching full monomer conversion within 8 min at 0.1 mol % of catalyst loading and in 35 min at 0.01 mol % of catalyst loading. Catalysts **12** and **13** displayed conversions and *E*/*Z* ratios very similar to those for **2a** and **3a** under identical reaction conditions (Figure 7, Table 1). These results underline the negligible role of both reduced bulk at the *ortho* positions of *N*-aryl groups and different stereochemical arrangement of substituents on the backbone of the NHC ligand in addressing activity and stereoselectivity in the ROMP of COD.

Finally, we examined the catalytic activity of **12** and **13** in the representative cross-metathesis reaction of allyl benzene (**23**) and *cis*-1,4-diacetoxy-2-butene (**24**), illustrated in Scheme 5. Both the catalysts showed good conversions to desired heterocoupled product **25**, with *E*/*Z* ratios comparable to those of **2a** and **3a**, revealing also in this reaction scarce influence of the backbone substitution as well as of the substitution on the *N*-aryl groups.

Conclusions

We have reported the preparation and characterization of two novel ruthenium complexes (**12** and **13**) containing N-heterocyclic carbenes with *syn* and *anti* arrangement of methyl substituents on the backbone and *o*-tolyl groups at the nitrogen atoms. The catalytic performance of these complexes was tested in RCM, ROMP, and CM reactions, displaying activities very similar to most of the existing Grubbs second-generation catalysts. Of particular interest, catalyst **12** was revealed to be the most efficient monophospine Ru catalyst known in the RCM reaction leading to tetrasubstituted olefins. As a consequence of a preferential *syn* orientation adopted by the *N*-tolyl rings, the high reactivity observed for catalyst **12** can be attributed to accessibility of conformations in which the *N*-aryl rings are rotated away from approaching and coordinated olefins, in order to better accommodate hindered substrates. To the best of our knowledge, this is the first time that separated *syn* and *anti* backbone-substituted NHC Ru complexes with *N*-aryl groups are compared in olefin metathesis reactions. Work is in progress in order to test **13** in asymmetric ring-closing metathesis as well as to extend our investigation to new ruthenium complexes with NHC ligands bearing *syn* and *anti* methyl groups on the backbone and a variety of *N*-substituents.

Moreover, a novel tris(piridyne) Ru complex **15** arising from the decomposition via C−H activation of the *N*-tolyl group of **12** in the presence of pyridine has been reported.

Experimental Section

All reactions involving metal complexes were performed under a nitrogen atmosphere using standard Schlenk techniques and glovebox techniques with solvents being distilled over standard drying agents and degassed before use. Deuterated solvents were dried and stored over 4 Å molecular sieves. All chemical products were purchased from Sigma-Aldrich Company and were reagent quality. These products were used without further purification. Diamines **6** and **7**,[10] as well as dienes **18** and **20**,[24] were synthesized according to literature procedures.

Flash column chromatography of organic compounds was performed using silica gel 60 (230−400 mesh). Silica gel for the purification of organometallic complexes was obtained from TSI Scientific, Cambridge, MA (60 Å, 230−400 mesh, pH 6.5−7.0). Analytical thin-layer chromatography (TLC) was performed using silica gel 60 F254 precoated plates (0.25 mm thickness) with a fluorescent indicator. Visualization of TLC plates was performed by UV light and $KMnO_4$ or I_2 stains. All deuterated solvents were degassed under an N_2 flow and stored over activated molecular sieves (4 Å) in a glovebox prior to use. NMR spectra were recorded on a Bruker AM300 and a Bruker AVANCE 400 operating at 300 and 400 MHz for ^1H, respectively. The ^1H and ^{13}C NMR chemical shifts are referenced to $SiMe_4$ (δ = 0 ppm) using the residual protio impurities of the deuterated solvents as internal standard. ^{31}P NMR spectra were referenced using H_3PO_4 (δ = 0 ppm) as an external standard. Spectra are reported as follows: chemical shift (δ ppm), multiplicity, coupling costant (Hz), and integration. Multiplicities were abbreviated as follows: singlet (s), doublet (d), triplet (t), quartet (q), multiplet (m), and broad (br). The ^{13}C NMR

(22) Stewart, I. C.; Benitez, D.; O'Leary, D. J.; Tkatchouk, E.; Day, M. W.; Goddard, W. A.III; Grubbs, R. H. *J. Am. Chem. Soc.* **2009**, *131*, 1931–1938.

(23) Costabile, C.; Cavallo, L. *J. Am. Chem. Soc.* **2004**, *126*, 9592–9600.

(24) Kirkland, T. A.; R. H. Grubbs, R. H. *J. Org. Chem.* **1997**, *62*, 7310–7318.

(25) Chatterjee, A. K.; Choi, T.-L.; Sanders, D. P.; Grubbs, R. H. *J. Am. Chem. Soc.* **2003**, *125*, 11360–11370.

assignments were confirmed by two-dimensional correlation experiments (HSQC).

General Procedure for the Preparation of Rutenium Complexes 12 and 13. In a glovebox, a 50 mL flask was charged with imidazolinium salt (1.2 equiv) and potassium hexamethyldisilazide (1.2 equiv) in toluene. The reaction mixture was stirred at room temperature for 30 min; then $(PCy_3)_2Ru(=CHPh)Cl_2$ (1 equiv) was added and stirring was continued for 1.5 h at room temperature. After this time, the reaction mixture was concentrated and purified by flash column silica gel chromatography to afford the desired ruthenium catalyst as a powder.

Ruthenium Compound 12. Following the general procedure above, **10** (210 mg, 0.66 mmol), potassium hexamethyldisilazide (132 mg, 0.66 mmol), and $(PCy_3)_2Ru(=CHPh)Cl_2$ (453 mg, 0.55 mmol) in 6 mL of toluene afforded 250 mg (55%) of a green-brown powder (1:9 to 1:1 Et_2O in pentane).

^{1}H NMR (400 MHz, CD_2Cl_2): δ 19.06 (br s, Ru=C*H*Ph), 8.25 (d), 7.38−7.34 (m), 7.10 (m), 6.38 (br m), 4.48 (m), 4.38 (br m), 4.14 (br m), 2.65 (s) 2.60 (s) 2.51−0.89 (several peaks). ^{13}C NMR (100 MHz, C_6D_6): δ 298.66 (br s, Ru=*C*HPh), 297.15 (s, Ru=*C*HPh), 221.6 (d, J(P,C) = 78.0 Hz, *i*N*C*N), 218.3 (br d, J(P,C) = 79.5 Hz, *i*N*C*N), 152.2, 151.5, 140.3, 139.3, 139.0, 138.3, 137.9, 136.8, 135.7, 133.6, 132.5, 131.9, 131.0, 130.5, 127.1, 126.2, 65.2, 62.6, 61.4, 36.5, 35.9, 33.4, 33.3, 30.5, 29.5, 28.4, 27.5, 27.1, 20.8, 20.3, 20.0, 19.5. ^{31}P NMR (161.97 MHz, C_6D_6): δ 27.6, 25.1, 23.2. Anal. Calcd (%) for $C_{44}H_{63}Cl_2N_2PRu$ (822.93): C 64.22, H 7.72, N 3.40. Found: C 64.18, H 7.65, N 3.42.

Ruthenium Compound 13. Following the general procedure above, **11** (200 mg, 0.63 mmol), potassium hexamethyldisilazide (131 mg, 0.66 mmol), and $(PCy_3)_2Ru(=CHPh)Cl_2$ (443 mg, 0.54 mmol) in 6 mL of toluene afforded 270 mg (61%) of a brown powder (1:9 to 1:1 Et_2O in pentane). ^{1}H NMR (400 MHz, CD_2Cl_2): δ 19.05 (s, Ru=C*H*Ph), 19.02 (br s, Ru=C*H*Ph), 8.19 (br s), 7.36 (m), 7.08 (t), 6.71 (t), 4.04 (br m), 3.77 (br m), 3.66 (br m), 2.6 (s), 2.18 (br s), 1.96 (d), 1.76−0.87 (several peaks). ^{13}C NMR (100 MHz, C_6D_6): δ 295.8 (s, Ru=*C*HPh), 218.6 (d, J(P,C) = 78.8 Hz, *i*N*C*N), 151.8, 140.6, 139.5, 139.3, 137.5, 137.1, 135.3, 133.0, 131.8, 130.8, 129.9, 127.3, 126.8, 126.1, 72.0, 70.7, 66.4, 66.1, 65.5, 33.3, 33.2, 29.7, 29.6, 28.4, 27.0, 20.4, 20.2, 20.1, 19.8. ^{31}P NMR (161.97 MHz, C_6D_6): δ 26.6, 24.2. Anal. Calcd (%) for $C_{44}H_{63}Cl_2N_2PRu$ (822.93): C 64.22, H 7.72, N 3.40. Found: C 64.20, H 7.66, N 3.45.

Ruthenium Compound 15. To a toluene solution of **12** (100 mg, 0.12 mmol) was added an excess of pyridine (0.80 mL), and the reaction mixture was stirred at room temperature for 30 min. A color change of solution from brown to bright green was observed. Fifteen milliliters of pentane was added, and the solution was left at room temperature for 12 h. After this time, the color of the solution changed from green to brilliant red, and a white solid precipitated. The red solution was decanted away from the white precipitate and cooled at −20 °C. Precipitation of the red crystalline solid was observed after 48 h. The solid was filtered, washed with pentane, and dried under vacuum to provide **15** as a red-orange solid (29.9 mg, 32%). ^{1}H NMR (300 MHz, C_6D_6): δ 9.55 (d); 9.29 (d), 8.91 (d), 8.55 (dd), 7.39 (d), 7.12−6.16 (several peaks), 4.28 (m), 3.93 (br s), 3.48 (m), 2.76 (s), 2.69 (s), 2.56 (s), 1.02 (d), 0.70 (d). Anal. Calcd (%) for $C_{41}H_{44}Cl_2N_5Ru$ (778.8): C 63.23, H 5.69, N 8.99. Found: C 63.20, H 5.71, N 9.03.

RCM of Diethyldiallylmalonate (16, Figure 4, Table 1). An NMR tube with a screw-cap septum top was charged with 0.80 mL of a CD_2Cl_2 solution of catalyst (0.80 μmol). After equilibrating at the appropriate temperature the sample in the NMR probe, 19.3 μL (0.080 mmol) of **16** was injected into the tube. The reaction was monitored as a function of time, and the conversion to **17** was determined by integrating the methylene protons in the starting material, δ 2.61 (dt), and those in the product, δ 2.98 (s).

RCM of Diethylallylmethallylmalonate (18, Figure 5, Table 1). An NMR tube with a screw-cap septum top was charged with 0.80 mL of a CD_2Cl_2 solution of catalyst (0.80 μmol). After equilibrating at the appropriate temperature the sample in the NMR probe, 20.5 μL (0.080 mmol) of **18** was injected into the tube. The reaction was monitored as a function of time, and the conversion to **19** was determined by integrating the methylene protons in the starting material, δ 2.67 (s), 2.64 (dt), and those in the product, δ 2.93 (s), 2.88 (m).

RCM of Diethyldimethallylmalonate (20, Figure 6, Table 1). An NMR tube with a screw-cap septum top was charged with 0.80 mL of a CD_2Cl_2 solution of catalyst (4.0 μmol). After equilibrating at the appropriate temperature the sample in the NMR probe, 21.6 μL (0.080 mmol) of **20** was injected into the tube. The reaction was monitored as a function of time, and the conversion to **21** was determined by integrating the methylene protons in the starting monomer, δ 2.71 (s), and those in the product, δ 2.89 (s).

ROMP of COD (22, Figure 7, Table 1). An NMR tube with a screw-cap septum top was charged with 0.80 mL of a CD_2Cl_2 solution of catalyst (0.40 μmol). After equilibrating at 30 °C the sample in the NMR probe, 49.1 μL (0.40 mmol) of **22** was injected into the tube. The polymerization was monitored as a function of time, and the conversion to poly(**22**) was determined by integrating the methylene protons in the starting monomer, δ 2.36 (m), and those in the product, δ 2.09 (br m), 2.04 (br m).

CM of Allylbenzene (23) and *cis*-(1,4)-Diacetoxy-2-butene (24) (Table 1). A 55 μL amount of **23** (0.5 mmol) and 160 μL of **24** (1.0 mmol) were added simultaneously via syringe to a stirring solution of catalyst (0.013 mmol) in 2.5 mL of CH_2Cl_2. The flask was refluxed under nitrogen for 12 h. The reaction mixture was concentrated and purified directly on a silica gel column (9:1 hexane/ethylacetate). **25** was obtained as a pale oil. *E*:*Z* ratio was determined by integration of peaks at δ 4.73 and 4.55.

Acknowledgment. The authors thank Patrizia Oliva and Dr. Mariagrazia Napoli of the Department of Chemistry of the University of Salerno for their technical assistance.

Supporting Information Available: Further synthetic details. This material is available free of charge via the Internet at http://pubs.acs.org or from the authors.